Geotechnical Engineering Journal of the SEAGS & AGSSEA Vol 42 No.2 June 2011 ISSN 0046-5828

Vertical Load Test and Settlement Analysis of Cast-In-Place Concrete Nodular Piles Supporting a High-Rise Building

N. Suzuki[1] and T. Seki[2]
[1]*Technical Research Institute, Obayashi Corporation, Tokyo, Japan, Corresponding Author,*
E-mail: suzuki.naoko@obayashi.co.jp
[2]*Technical Research Institute, Obayashi Corporation, Tokyo, Japan*

ABSTRACT: This paper describes full-scale pile load tests and 3D FEM settlement analyses regarding cast-in-place concrete nodular piles for design of a high-rise building foundation. The nodular piles have bulbs on its shaft in order to increase pile resistance.

A compressive & tensile load test and a tensile load test were carried out in the site of the high-rise building for design purpose. Each bulb of the test piles was installed in medium gravel layer and dense gravelly sand layer. Although load condition included repeated loading and long-term loading (4 days), the measured test results showed that resistance of the bulb was sufficient in both layers. Furthermore, concerning settlement behaviour of the bulb, it was attempted to normalize relationship between bearing pressure and settlement. As a result, the authors' normalization method worked well to evaluate settlement behaviour of the bulb.

With regard to analysis, 3D FEM analyses of pile group under sustained loading and earthquake loading were conducted. These analyses were based on the analyses of the two pile load tests. In the pile group analyses, settlement of the foundation and distributions of loads on the pile head were evaluated for design. The influence of load dispersion due to stiffness of the footing beams were considerably large and marked particularly under earthquake loading.

Keywords: Cast-in-place concrete nodular pile, Load test, FEM analysis, Pile group efficiency

INTRODUCTION

This paper describes an examination of a pile group foundation supporting a high-rise building under sustained loading and earthquake loading using static FEM analyses.

Many reports have already described about settlement behaviour of pile foundations supporting high-rise buildings under sustained loading. However, under earthquake loading, general design of pile foundation is only a check of the pile bearing capacity against compressive load and tensile load. Therefore, there are only few reports which describe the design method based on analyses of settlement behaviours of pile group foundations (Suzuki et al., 2009b).

In the high-rise building presented in this paper, cast-in-place concrete nodular piles are placed in the area where large axial loads act on the pile heads. The cast-in-place concrete nodular pile (hereafter, it is described as 'nodular pile') has bulb on its shaft in order to increase the pile resistance. In Japan, Hirai et al. (2008) and Sudo et al. (2008) have reported about development of the nodular pile.

For actual design of the building foundation, resistance of the bulb was examined using full-scale load tests of single piles in the construction site. Furthermore, applicability of FEM analysis was confirmed by simulating settlement behaviour of the load tests. Based on these analyses, the analysis method for single pile was applied to the design of pile group foundation.

OUTLINE OF BUILDING, SOIL AND FOUNDATION

Figure 1 shows the pile location plan, and Figure 2 shows a cross section of the building. The building is a 45-storey reinforced-concrete structure with 1 basement floor. The building has a rectangle shape of 40 m × 45 m in plan, 148 m in height, height-to-width ratio of 3.3 to 3.7. The average ground contact pressure due to the dead load of the building and live load is 528 kN/m^2. The building is composed of multi-storey shear-wall structure and main rigid-frame structure, and these two structures are connected by oil damper. In other words, there are two different rigidity structures in one building, and the two structures are connected by vibration control device. Such vibration control system is named 'Dual Frame System' (Nishimura et al., 2008).

Figure 3 shows the profiles of soil layers, SPT *N*-values and other soil investigation results. Medium gravel layer extends from the surface to a depth of about 25 m, dense gravelly sand of about 10 m in thick spreads under that, and there are multi-layer soil composed of hard clay and dense sand from about 35 m in depth to the deepest depth investigated. Bearing layer of pile tip is dense sand layer at GL-42 to 52 m in depth, and *N*-value of this layer is 50 or more. The bearing layer is inclined about 10 m in depth on the site so that lengths of piles are different. Nodular piles are placed at 10 locations where large axial loads act on the pile heads under sustained loading and earthquake loading. Bulb sections of the piles are installed in the dense gravelly sand around 30 m in depth.

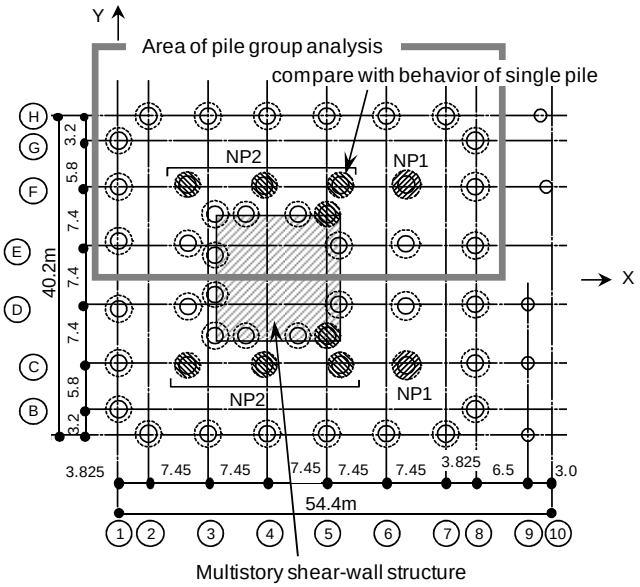

Symbol	Pile	Diameter of shaft (m)	Diameter of nodular part (m)	Diameter of belled part (m)
	Nodular pile (NP1)	2.2	3.2	3.6
	Nodular pile (NP2)	2.2	3.2	3.2
	Belled pile	2.1～2.2	-	3.3～3.6
	Straight pile	1.6	-	-

Figure 1 Pile location plan of building and area of pile group analysis

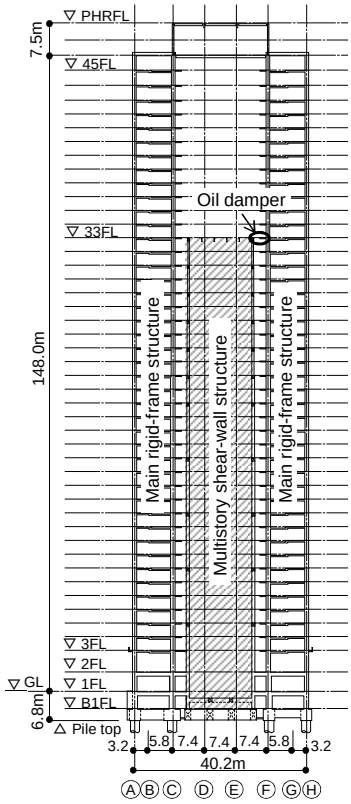

Figure 2 Cross section of building

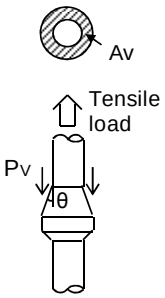

Av Annular projection area

Pv Bearing load of bulb (difference of axial force between upper of bulb and lower of bulb)

pv Bearing pressure of bulb (pv = Pv ÷ Av)

θ Tapered angle of bulb

Figure 4 Evaluation method of bearing pressure

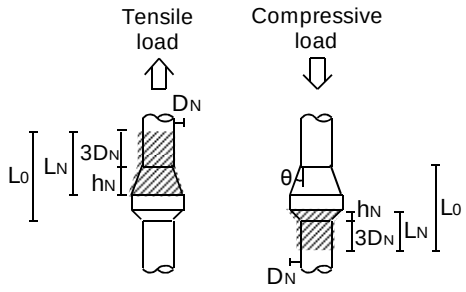

LN Length to use for evaluation of average N-value and average undrained shear strength

L0 Length to be neglected friction of pile for evaluation of pile capacity

DN Enlarged width

HN Enlarged height

θ Tapered angle of bulb

Figure 5 Evaluation method of bearing capacity

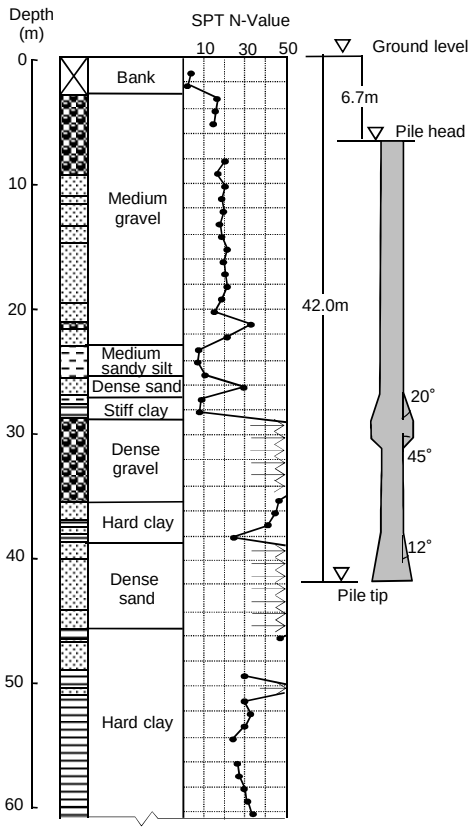

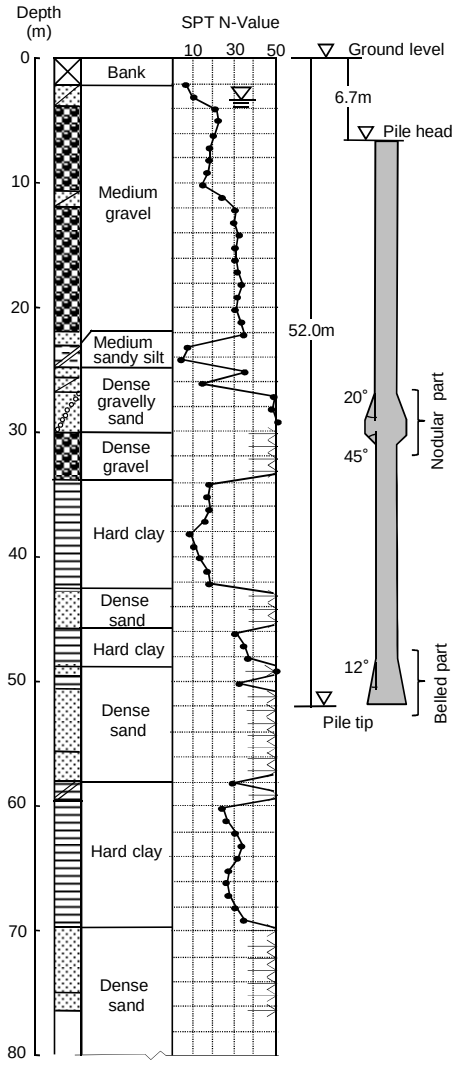

Vs (m/s)	Eps (MPa)	v	G/Go-γ	fmax (kN/m²)
178	177	0.30	Gravel	0
				66
221	243	0.45	Clay	100
258	337	0.30	Sand	66
347	725	0.30	Gravel	100
295	415	0.45	Clay	100
319	603	0.30	Sand	100
384	809	0.45	Clay	100
375	801	0.30	Sand	—
357	635	0.45	Clay	—
407	910	0.30	Sand	—

Vs Velocity of S-wave obtained from PS logging

Eps Elastic modulus obtained from PS logging

v Poisson's ratio used in the analysis of pile group

G/Go-γ Stiffness-strain relation used in the analysis of pile group, G: soil shear modulus at shear strain, Go: initial soil shear modulus at small strain level, γ: shear strain

fmax Ultimate unit frictional resistance used in the analysis of pile group

Figure 3 Soil profile, soil properties and installed depth of nodular piles in

OUTLINE OF ESTIMATION METHOD OF RESISTENSE ON BULB

Bearing capacity of bulb is estimated by means of a simplified method as shown in Figures. 4 and 5. The uplift bearing pressure, p_{vu}, of the annular projection area, A_v, of the bulb in sandy soils is calculated using Eq. (1).

Sandy soils: $p_{vu} = 100N$ ($N \leqq 60$, $p_{vu} \leqq 6000$ kN/m^2) (1)

where N is the average of SPT N-values around the bulb. This equation has been led from five full-scale tests in this paper and the previous papers (e.g. Sudo et al. 2008).

It is assumed that compressive bearing capacity of bulb is equal to the uplift bearing pressure of bulb regardless of loading direction. In addition, uplift bearing pressure of bell-shaped bulb at the pile tip is assumed to be equal to the uplift bearing pressure of the bulb at the pile shaft, because their bearing mechanisms are similar. Ultimate bearing capacity of the bulb is p_{vu} multiplied by A_v .

Shaft friction along a length of L_0 indicated in Figure 5 is neglected in pile design. Ultimate shaft friction, f_{max}, except for the section of L_0 is estimated using the following empirical equations:

Sandy soils: $f_{max} = 3.3N$ (kN/m^2) (2)
Clayey soils: $f_{max} = 6c_u$ (3)

where c_u is undrained shear strength of clayey soils. These equations have been specified in Notification No. 1113 of the Ministry of Land, Infrastructure and Transport (2002).

LOAD TESTS OF SINGLE PILES

Specifications of Test Piles

Two load tests, compressive & tensile load test and tensile load test, were carried out on two separate single piles in the site. Figure 6 shows the soil profile together with seating of the test piles. Table 1 lists specifications of the test piles and maximum loads.

In the case of the compressive & tensile load test on pile No. 2, a bulb was constructed in the medium gravel layer having SPT N-value of about 20, and the pile tip was located in the dense gravelly sand layer having N-value of 45. The pile No. 2 was designed to

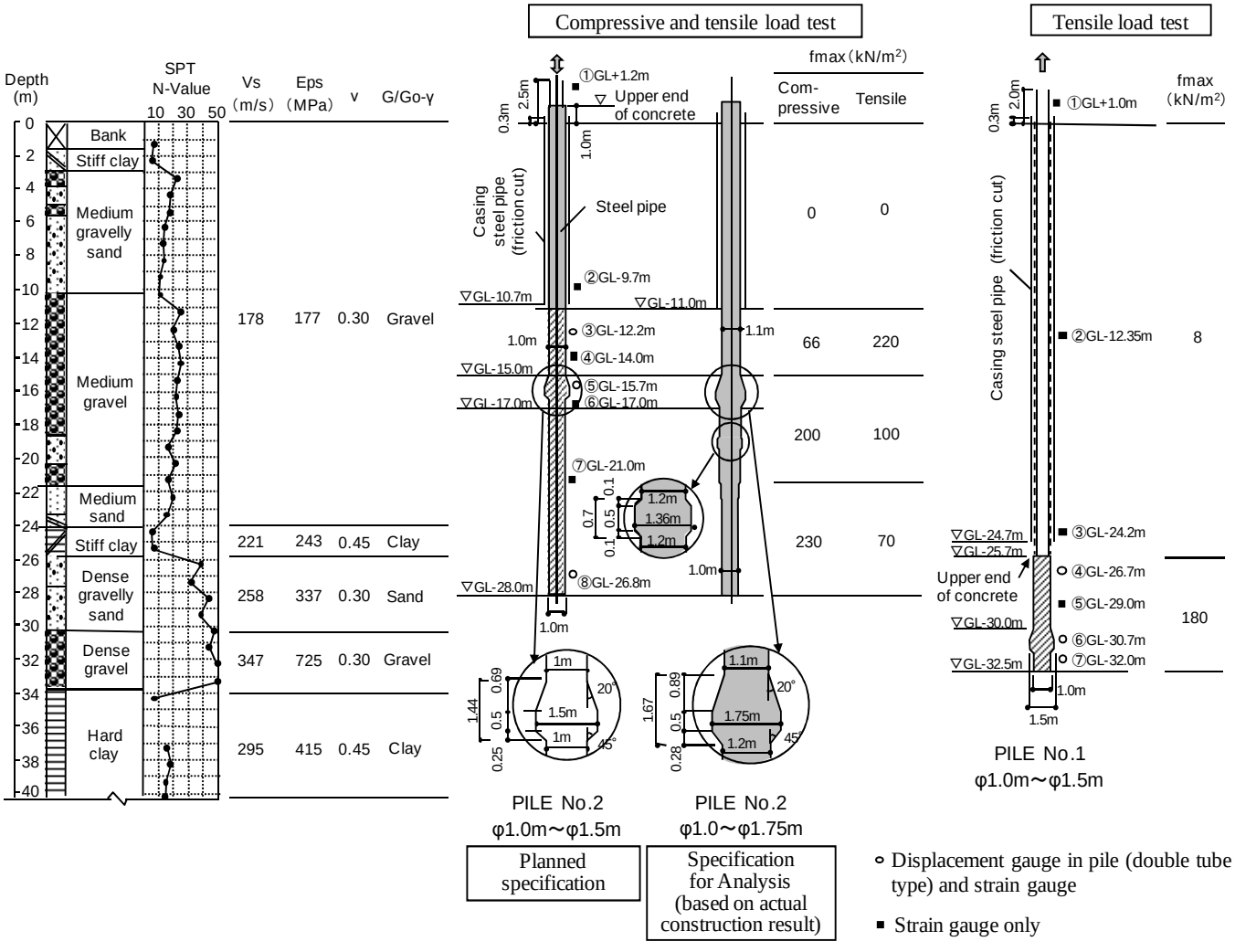

Vs	Velocity of S-wave obtained from PS logging
Eps	Elastic modulus obtained from PS logging
ν	Poisson's ratio for analysis of pile group
G/Go-γ	Stiffness-strain relation for analysis of pile group, G: soil shear modulus at shear strain, Go: initial soil shear modulus at small strain level, γ: shear strain
fmax	Ultimate unit frictional resistance for analysis based on result of pile load test

Figure 6 Soil profile, soil properties and installed depth of nodular piles in load

have a bulb having a diameter of 1.5 m and uniform cross-section, 1.0 m in diameter, for the other sections. However, the constructed pile had a little of different configuration as shown in Fig. 6 due to collapse of the borehole walls. Note that friction cut using a casing steel pipe pile was done to a depth of 11 m below the ground surface.

In the case of the tensile load test on pile No. 1, a bulb was constructed in the dense gravelly sand layer having *N*-value of about 45. The bulbs of the nodular piles used in the building were constructed also in this layer. Test pile No. 1 having a length of 6.8 m was constructed below a depth of 25.7 m, in order to confirm the maximum uplift resistance of the bulb within the loading capacity of the loading system employed. Pre-stressing steel bars were connected to the pile head to apply tensile loads. The pre-stressing steel bars were protected by a casing steel pipe pile. The casing pipe was filled with gelling slurry for cutting friction.

Test Method

The two load tests were carried out following the Standards for Vertical Load Test of Piles (Japanese Geotechnical Society, 2002). As shown in Fig. 7, loading method employed was stepwise and multi-stage loading method including long-term loading (4 days) and repeated loading.

Test Results

Figure 8 shows the measured relationships between load and displacement obtained from the two load tests. The measured maximum loads were approximately twice as much as the values estimated in the design stage (*see* Table 1). In the tensile load test, the uplift bearing pressure of the bulb was 7500 kN/m^2. This value sufficiently exceeds the value from Eq. (1). As mentioned previously, the depth of the bulb of the test pile No. 1 is the same as that of the working piles constructed for the high-rise building.

It can be seen from Fig. 8 that the difference between the displacements at the pile head and the pile tip was small in both load tests. During the repeated loading, the displacement accumulated. This tendency became pronounced as the load intensity became larger. In addition, concerning distributions of axial force, influence due to repeated loading and long-term loading has been considerably small. Other results of the tests will be presented and discussed later with the results of FEM analyses of the load tests (*see* Figs. 12 to 17).

Table 1 Specifications of test pile and maximum load

	Diameter of shaft (m)	Diameter of nodular part (m)	Depth of pile top (m)	Depth of pile tip (m)	Maximum compressive load (kN)	Maximum tensile load (kN)
Compressive & tensile load test	1.0	1.5	11.0	28.0	16,000 (9,000)*	9,990 (5,500)*
Tensile load test	1.0	1.5	25.7	32.5	—	10,000 (5,000)*

(*Expected maximum resistance before load test)

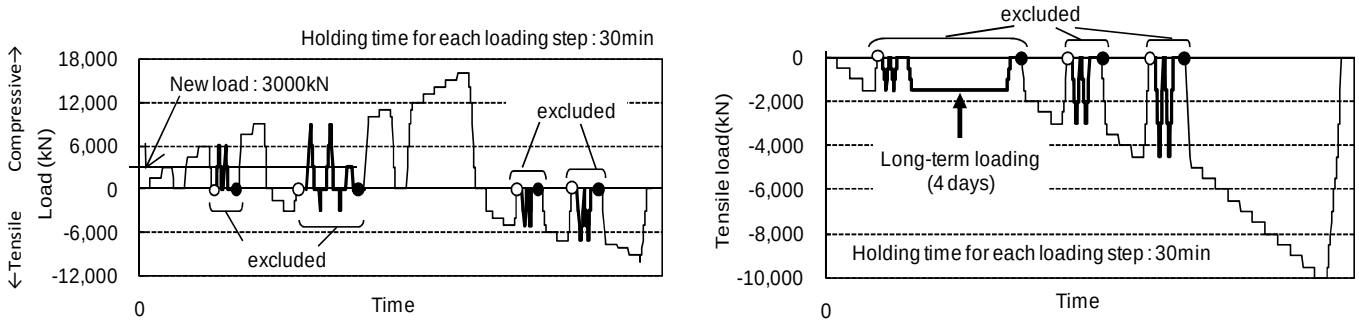

(a) Compressive and tensile load test (b) Tensile load test

Figure 7 Load-time relationship of load tests and excluded range for comparison with analysis result

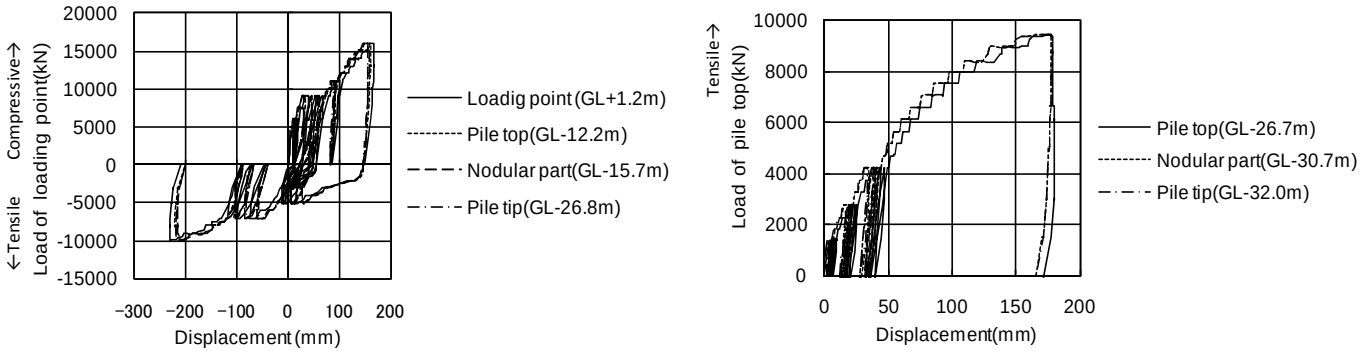

(a) Compressive and tensile load test (b) Tensile load test

Figure 8 Relationship between load and displacement of each part

Modelling Method of Simulation Analysis

In this paper, FEM analyses were carried out using a commercial finite element analysis software SoilPlus (2008). Figure 9 shows the FEM model for simulation of the compressive & tensile load test as an example. In the FEM analysis of the single pile, one-quarter of the pile and the surrounding ground was modelled.

The ground was modelled by nonlinear elastic solid elements. Strain dependency of the soil was considered using G/G_o versus γ (Fig. 10) that is specified in the Recommendations for Design of Building Foundations (2001). Here, G_0 is initial soil shear modulus at small strain level, G is soil shear modulus at shear strain, γ. The initial shear modulus, G_0, was obtained from PS logging (elastic wave investigation) in this research.

The pile under compressive loading was modelled with linear elastic solid elements, and the pile under tensile loading was modelled with non-linear elastic solid element. The stress-strain relationship of the nonlinear element is given as shown in Fig. 11. This stress-strain relationship considers cracks caused in concrete due to tensile stress based on Naganuma et al. (1990) in which the non-linear responses of reinforced concrete were obtained from tensile load tests of the reinforced concretes. As for the diameter of shaft and bulb of test pile No. 2 used in the analysis, the size based on actual construction result was adopted due to collapse of the borehole wall (*see* Fig. 6). In the case of pile No. 1, the section of pre-stressing steel bars was modelled with elasticity solid element having a diameter of 1.0 m. Its elastic modulus was equivalent for the axial rigidity of the pre-stressing steel bars.

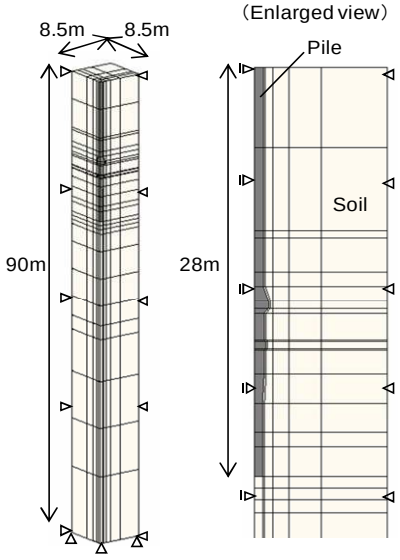

Figure 9 FEM model for simulation analysis of compressive & tensile load test

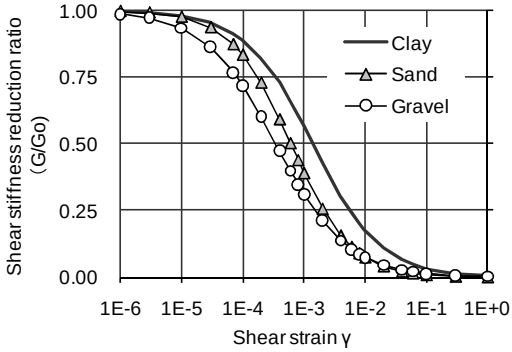

Figure 10 Relationship between Shear stiffness reduction ratio and shear strain

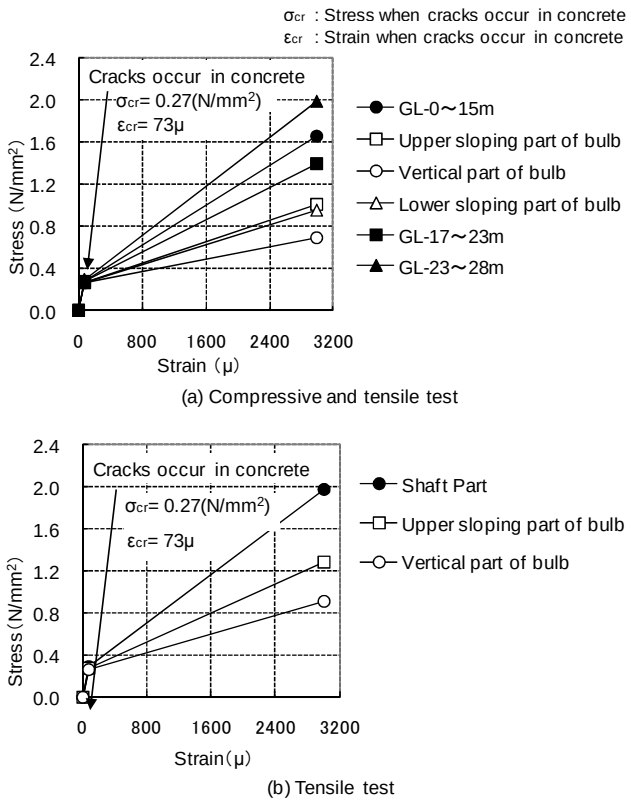

Figure 11 Stress-strain relationship of pile under tensile load acts used in simulation analysis of load tests

Interface elements were arranged on the pile surface. The shaft resistance of the pile in the compressive & tensile load test was modelled as rigid perfectly-plastic response by using a very large shear stiffness of the interface elements (e.g. Suzuki et al., 2009a). The maximum shaft resistance, f_{max}, were determined from the measured values shown in Fig. 6. That is, cohesion type of shaft resistance was adopted.

In contrast, in the analysis of the tensile load test, a bi-linear response of the interface element was finally adopted so that good simulation results could be obtained. Concretely, its yield stress, f_{max}, and yield relative displacement between the ground and pile shaft were defined 180kN/m^2 and 180mm, respectively. Consequently, the initial shear stiffness of the interface element was 1000kN/m^3 and the shear stiffness after yielding was set to 1/10,000 times the initial stiffness.

Furthermore, tension cut type interface elements were used at lower and upper sloping of the bulb and the pile tip.

Load on the pile top was gradually increased up to the maximum load. Compressive load test and tensile load test were successively carried out on pile No. 2. However, analyses of these load test stages were conducted separately with the same initial conditions at zero load.

Although repeated loading was adopted in the load tests on piles No. 1 and No. 2 as shown in Fig. 7, the responses of the test piles subjected to monotonic loading were analysed in the FEM analyses.

Comparison of Test and Analysis Results

Test and analysis results of the compressive & tensile load test on pile No. 2 are compared in Figs. 12 to 14. The FEM analysis simulates well the measured results of the axial force versus displacement at pile head (Fig. 12) and distributions of axial forces (Fig. 13). However, with respect to the bearing pressure versus displacement of the bulb curve (Fig. 14), the analysis results are slightly different from the measured results when the tensile load is in small level. The reason of this difference may be that the analysis

model disregards the soil disturbance during the compressive loading conducted prior to the tensile loading.

Test and analysis results of the tensile load test on pile No. 1 are compared in Figs. 15 to 17. It can be seen from these figures that the FEM analysis simulates the test results very well.

Normalized Relationship between Bearing Pressure and Displacement

With regard to relationship between bearing pressure and pile tip displacement of cast-in-place concrete piles, Yamagata and Ito (1991) have proposed a normalized relation curve on the basis of field load test data. They collected load test data of piles installed in gravel or sandy soils. Similarly, Mochida and Moriwaki et al. (2000) have proposed two normalized curves for gravel and sand, in conjunction with the study group of Building Constructors Society (BCS). They collected field load test data, and obtained the normalized curves as shown in Fig. 18. In Fig. 18, p is bearing pressure, p_u is ultimate bearing pressure, S is displacement and D is diameter of pile or bulb. The ultimate bearing pressure, p_u, is determined as bearing pressure at a displacement of 0.1D.

The bearing pressures of the bulbs obtained from the load tests

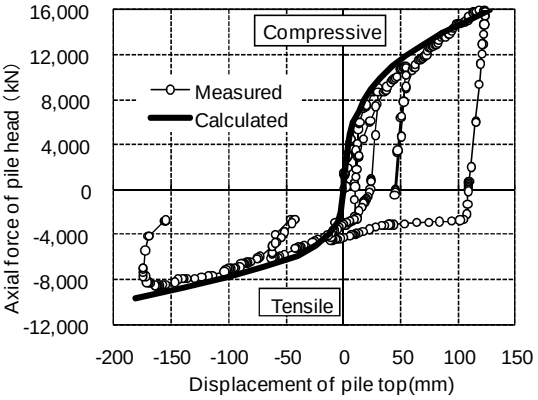

Figure 12 Axial force versus displacement at pile head: GL-10m (Compressive & tensile load test)

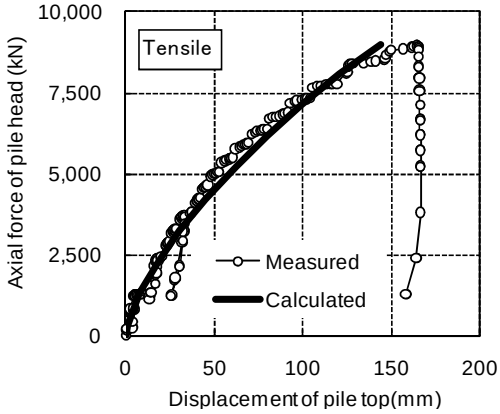

Figure 15 Axial force versus displacement curves at pile head (Tensile load test)

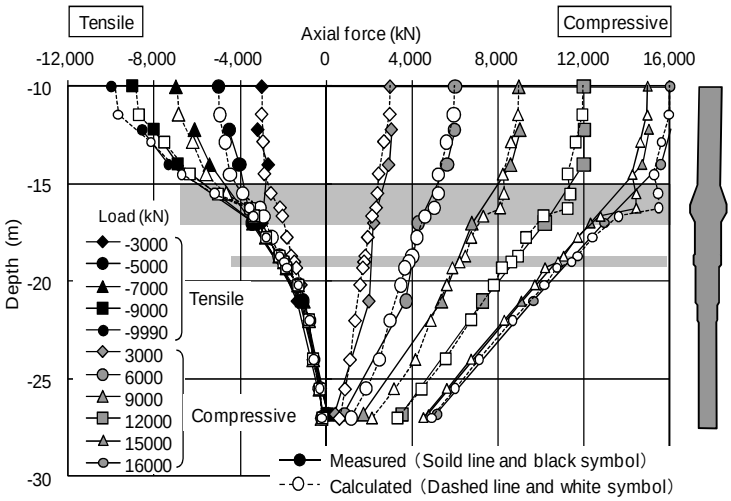

Figure 13 Distributions of axial forces of pile with depth (Compressive & tensile test)

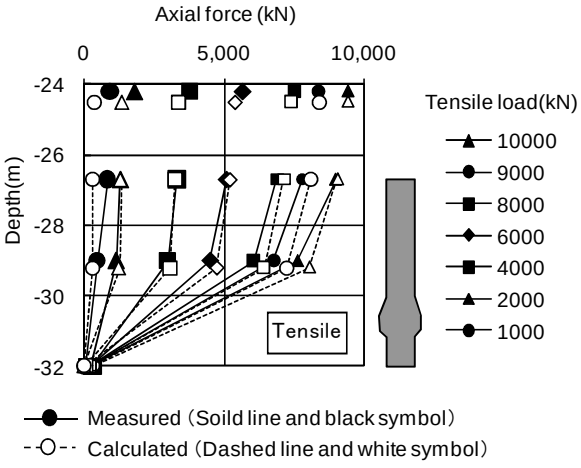

Figure 16 Distributions of axial forces of pile with depth (Tensile load test)

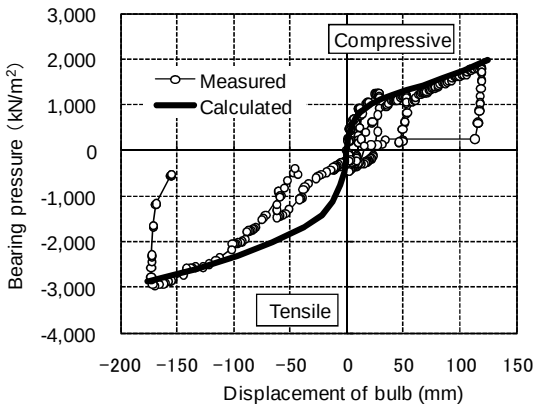

Figure 14 Bearing pressure versus displacement of bulb (Compressive & tensile load test)

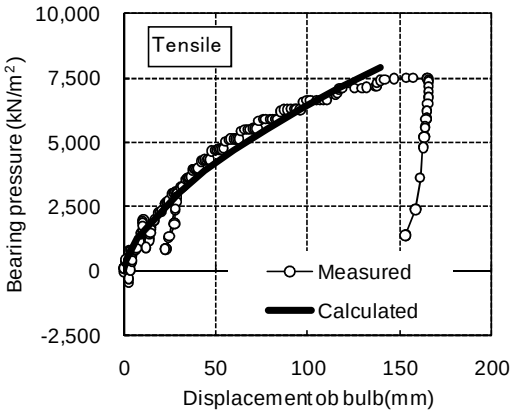

Figure 17 Bearing pressure versus displacement of bulb (Tensile load test)

are plotted in Fig. 18: (a) compressive bearing pressure of the bulb in gravelly soil measured in compressive loading in the compressive & tensile load test and (b) tensile bearing pressure of the bulb in gravelly sandy soil measured in the tensile load test.

Concerning with case (a), because the maximum displacement did not reach 10% of diameter of bulb (175 mm), displacement and bearing pressure at S = 175 mm were extrapolated using second-order polynomial approximation curve.

The measured curve in case (a) exhibits stepping down at S/D = 0.35. This seems to be caused by the influence of soil disturbance due to repeated loading. Nevertheless, in general, it can be seen that the bearing pressure versus displacement of the bulbs measured in the load tests are within the range of the previously proposed three curves.

ANALYSIS OF PILE GROUP

As mentioned above, it was confirmed that the adopted FEM modelling is capable for simulating the two pile load tests reasonably. Hence, the analytical method was applied to the settlement analysis of the pile group foundation for the building (*see* Figs. 1 to 3).

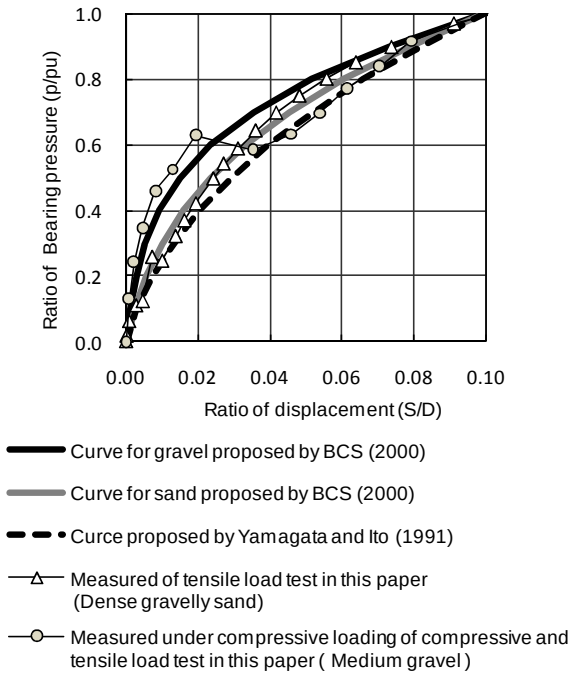

Figure 18 Normalized relationship between bearing pressure and pile displacement

The FEM analyses were carried out for sustained loading and earthquake loading. Note that earthquake loads were expressed by equivalent static loads in the analysis instead of without conducting dynamic analyses.

The purpose of the analyses was to estimate the following two effects: a) effect of pile group and b) effect of rigidity of footing beams on load dispersion.

Modelling Method

Half of the pile group foundation and the surrounding ground were modelled as shown in Fig. 19, because of symmetric conditions of the foundation and the ground. The inclined bearing layer for the pile tip was modelled according to the actual soil situation. Depth of its upper surface ranges from GL-42 m to -52 m, inclining from line 8 toward line 1 in pile location area as shown in Fig. 1.

The ground was modelled with nonlinear solid element having similar properties used in the analyses of the pile load tests mentioned previously.

Piles were modelled with linear solid elements, because it was judged that concrete cracks would not occur according to the following reason. Even though tensile loads act on piles located in the centre of the building under earthquake loading, loads would be dispersed due to high-rigidity of footing beams. The judgement will be validated later through the analysis results.

Footing beams were modelled with elastic beam elements. Their bending stiffness and shear stiffness included stiffness of shear-wall on the basement floor. The interface elements were used for the interface between the footing beams and the ground surface so as not to transmit tensile load from the footing beams to the ground.

Interface elements having a rigid perfectly plastic response were arranged on the pile surface, similar to the FEM analysis of the compressive & tensile load test on the test pile No. 2. The maximum shaft resistance, f_{max}, prescribed in the Notification No. 1113 of the Ministry of Land, Infrastructure and Transport (2002) (*see* Eqs. (2) and (3)) was used for design purpose. Tension cut was considered at lower and upper sloping of the bulb, the pile tip and the bottom of the pile.

The soil layer between the ground surface and 20 m in depth is liquefiable under earthquake loading. Hence, pile shaft resistance in this layer was disregarded under sustained loading and earthquake loading for design purpose.

Figure 20 shows the distributions of loads on the pile head in analysis of sustained loading (Fig. 20(a)) and in analysis of earthquake loading (Fig. 20(b)). The loads of the pile heads from the building were calculated separately using a frame analysis without piles.

In analysis of earthquake loading, a pseudo-static analysis was adopted. Horizontal seismic load was evaluated from the non-linear earthquake response analysis using a multi-mass-spring model.

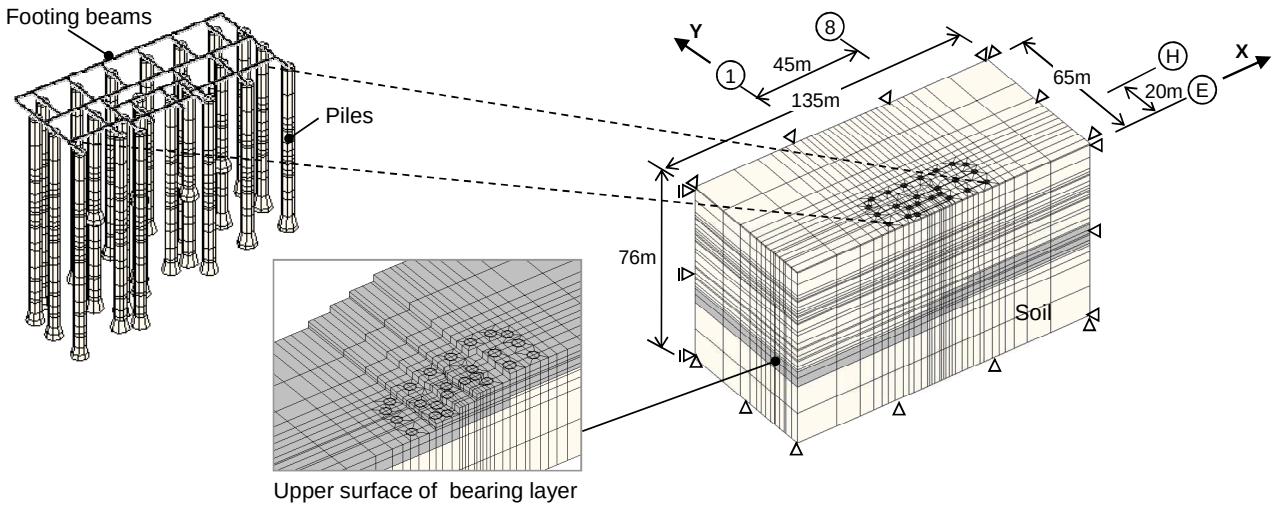

Figure 19 FEM model of pile group foundation and

From this analysis, equivalent horizontal load and overturning moment from the building were 77.5 MN and 3945.7 MNm, respectively. Here, horizontal seismic shear coefficient was *C*i = 0.091. The loads of the pile heads were calculated using a frame analysis without piles considering these external loads.

It is seen form Fig. 20(b) that large axial loads act over the area of multi-storey shear-wall structure at the centre of the building due to earthquake load. This is structural characteristics of the building using the Dual Frame System.

In order to investigate the effects of footing beams, two analyses were carried out with and without footing beams in cases of sustained loading and earthquake loading.

Result of Analysis about Settlement Behaviour

Figure 21 shows the calculated distributions of the pile head displacements in case of sustained loading (Fig. 21(a)) and in case of earthquake loading (Fig. 21(b)). Two calculated results with and without footing beams are shown in each figure.

In case of the sustained loading, the distribution of the foundation settlements takes a typical dish shape in cases of without and with footing beams. Average settlements are 21 mm and 20 mm in the former and the latter cases, respectively, indicating that the footing beams slightly reduce the average settlement. It is also seen that the footing beams reduces the bending deformation effectively.

In the earthquake loading (Fig. 21(b)), a very large inclination occurs along E-F section where the multi-storey shear-wall structure is located in case of without the footing beams. Uplift displacement is caused along this section. The maximum settlement attains to 85 mm. In case of with the footing beams, the average settlement and the differential settlement are effectively reduced.

The footing beams are used for the actual foundation. The calculated maximum settlement and maximum distortion angle are 24 mm and 1/1780 under sustained loading, and 38 mm and 1/690 under earthquake loading. These results satisfy the design criteria.

As mentioned above, the footing beams are very effective to reduce the average settlement and the differential settlement of the foundation. The footing beams, however, have harmful effects on the foundation at the same time. For example, large stresses are caused in the footing beams and the shear-wall. It should be noted that load distribution on the pile heads is influenced by the change of rigidity of the foundation. Hence, feed-back design procedure is needed to obtain an optimal design.

Effect of Pile Group

In order to investigate pile group effects, FEM analyses of a single pile under sustained loading and earthquake loading were carried out. The target single pile is located at the centre of the building where nodular piles are constructed with a minimum pitch of 1.2 times the diameter of the bulb (*see* Fig. 1). The loads applied to the singe pile were equal to those in the pile group analyses.

Figure 22 compares the distributions of axial forces in the single pile and the corresponding pile in the pile group for cases of sustained loading and earthquake loading. Pile group effects are clearly seen from the figure, i.e. the shaft resistance along the lower section of the pile in the pile group is lower than the shaft resistance of the single pile, although larger end-bearing resistance is mobilized in the pile group. Here, the settlements of the pile in the

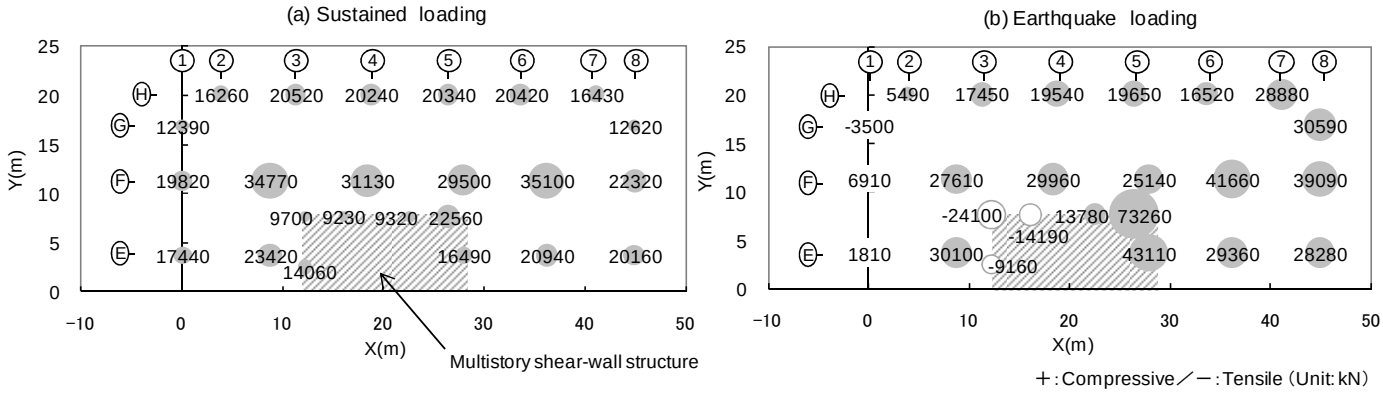

Figure 20 Distributions of load at pile

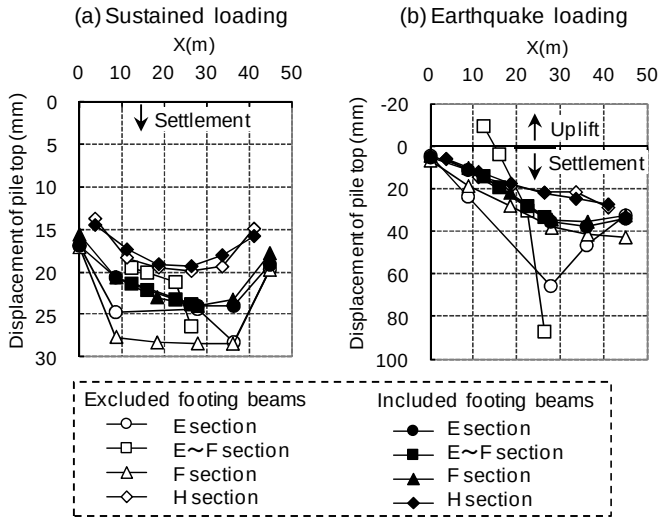

Figure 21 Distributions of displacement at pile

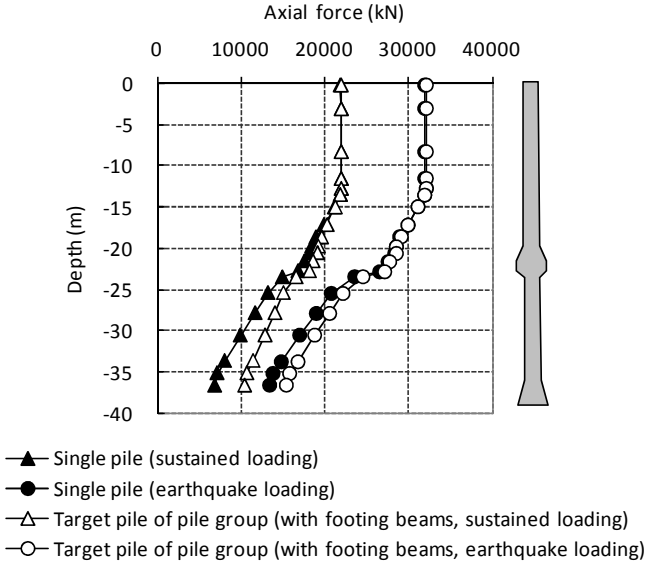

Figure 22 Distributions axial force along pile

pile group are 24 mm and 35 mm in cases of sustained loading and earthquake loading, respectively, which are greater than those of the single pile, 9 mm and 15 mm as shown Fig. 23.

The resistance of bulb (difference of axial forces between upper and lower sections of the bulb) in the pile group is approximately 80% of the resistance of the bulb in the single pile, indicating that

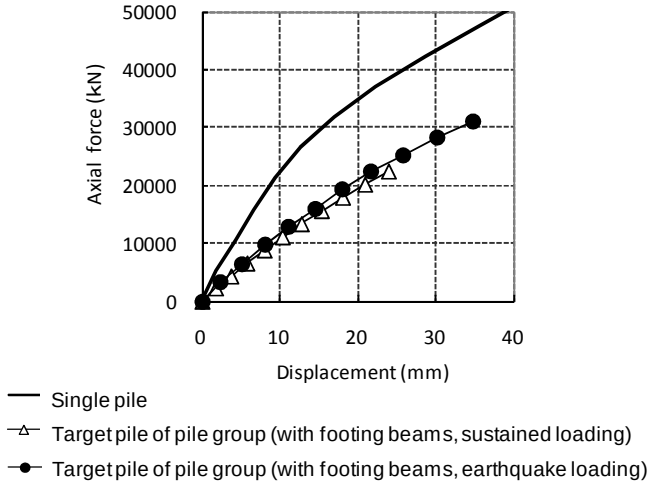

Figure 23 Axial force versus displacement curves at pile

the resistance of the bulb can be sufficiently expected in the pile group.

CONCLUSIONS

This paper describes two full-scale pile load tests and 3D nonlinear FEM analyses regarding cast-in-place concrete nodular piles in a high-rise building. The conclusions of this paper are summarized as follows:

1) According to the compressive & tensile load test and the tensile load test on nodular piles in the site, the resistance of bulb of nodular pile is large enough in both medium gravel and dense gravelly sand, even if repeated loading is applied to the piles.
2) Relationship between bearing pressure of the bulb and the normalized displacement is similar to those proposed for the end-bearing pressure of cast-in-place concrete piles, if the diameter of the bulb is used for normalization of the displacement.
3) According to the results of FEM analyses of the pile group foundation under sustained loading and earthquake loading, the influence of load dispersion due to stiffness of footing beams was considerably large. This influence marked particularly under earthquake loading. Although tensile load acts on a part of piles, settlement occurs at all of the piles. It was also demonstrated that, in the congested area where minimum pile pitch is 1.2 times the diameter of bulb, the resistance of bulb of the piles in the pile group is approximately 80% of that of the single pile.

ACKNOWLEDGEMENTS

The authors thank Dr. F. Chatani for his great effort to accomplish this work. We thank Dr. K. Nishimura and Y. Fukumoto for their supports as well, who designed the building. Furthermore, we thank T. Sudo for providing us various data of the load tests.

REFERENCES

Architectural Institute of Japan (AIJ). (2001). Recommendations for Design of Building Foundations, p142.

HIRAI, Y. and AOKI, M. (2008). "In-Situ Pull-Out Tests on Uplift Resistance Behaviour of Cast-In-Place Concrete Pile with Bell Enlargement", *Journal of Structural Engineering*, Architectural Institute of Japan, vol.54B, pp 59-66.

Japanese Geotechnical Society (JGS). (2002). Standards for Vertical Load Test of Piles.

Ministry of Land, Infrastructure and Transport (2002). Notification No.1113.

MOCHIDA, S. and MORIWAKI, T. et al. (2000). "Bearing Capacity of Cast-in-place Concrete Pile: Part1", *Summaries of Technical Papers of Annual Meeting Architectural Institute of Japan*, Architectural Institute of Japan, B-1, pp 725-726.

NAGANUMA, K. and YAMAGUCHI, T. (1990). "Tension Stiffening Model under In-plane Shear Stress", *Proceedings of Int. Conference on Asian Geotechnical*, Architectural Institute of Japan, C, pp 649-650.

NISHIMURA et al. (2008). "Response Performance of Hi-rise Reinforced Concrete Building using Coupled Vibration Control Structure : Part1", *Summaries of Technical Papers of Annual Meeting Architectural Institute of Japan*, Architectural Institute of Japan, C-2, pp 859-860.

SoilPlus (2008). "Theory Manual of SoilPlus Static", ITOCHU Techno-Solutions Corporation.

SUDO, T. and CHATANI, F. et al. (2008). "Static Axial Reciprocal and Tensile Load Tests of Single Cast-in-place Concrete Nodular Piles (Part 1 - Part 5)". *Summaries of Technical Papers of Annual Meeting Architectural Institute of Japan*, Architectural Institute of Japan, B-1, pp 567-576.

SUZUKI, N. et al. (2009a). "Static Axial Tensile and Compressive Load Tests of Nodular Diaphragm Wall Supporting High-rise Tower: Part5", *Summaries of Technical Papers of Annual Meeting Architectural Institute of Japan*, Architectural Institute of Japan, B-1, pp 447-448.

SUZUKI, N. and SEKI, T. et al. (2009b). "Piled Raft Foundation Supporting High Building under Over-Turning Moment due to Earthquake", *Journal of Architecture and Building Science*, Architectural Institute of Japan, vol.15, No.29, pp 89-94.

YAMAGATA, K. and ITO, A. et al. (1991). "Statistical Study on Ultimate Point Load and Point Load-Settlement Characteristics of Cast-in-place Concrete Pile", *Journal of Structural and Construction Engineering*, Architectural Institute of Japan, No.423, pp 137-146.